Exploring the boundary of 3D perovskites domain: The case of $FAPb_{1-x}Sn_xBr_3$ perovskites

Ambra Pisanu,[a] *Arup Mahata,*[b,c] *Edoardo Mosconi,*[b,*] *Maddalena Patrini,*[d] *Paolo Quadrelli,*[a] *Chiara Milanese,*[a] *Filippo De Angelis,*[b,c,*] *Lorenzo Malavasi* [a,*]

[a]Department of Chemistry and INSTM, Viale Taramelli 16, Pavia, 27100 (Italy);

[b]Computational Laboratory for Hybrid/Organic Photovoltaics (CLHYO), CNR-ISTM, via Elce di Sotto 8, I-06123 Perugia, Italy

[c] D3-CompuNet, Istituto Italiano di Tecnologia, Via Morego 30, 16163 Genova, Italy

[d] Department of Physics and CNISM, Via Bassi 6, Pavia, 27100 (Italy)

Corresponding Authors

*Lorenzo Malavasi, email: lorenzo.malavasi@unipv.it; tel. +39 382 987921

*Edoardo Mosconi, Filippo De Angelis, email: edoardo@thch.unipg.it, filippo@thch.unipg.it

ABSTRACT

Organic-inorganic perovskites are one of the most promising photovoltaic materials to design the next generation of solar cells. Lead-based perovskite prepared with methylammonium and iodide was the first and still one of the most used for efficient solar cells. However, perovskites prepared using formamidinium (FA) A-site cation shows several interesting properties. While most of the FA-based perovskites absorbers in the literature are lead halides, few information are available when exploring the substitution of Sn for Pb in such compounds.

In this paper we carried out a joint experimental and computational investigation of the $FAPb_{1-x}Sn_xBr_3$ system (*i.e.*, $0 \leq x \leq 1$) finding out non-monotonic band-gap evolution along with the Sn content. This is due to the FA cation being too large to fit into the $SnBr_3$ cavity and inducing a quasi 0D structure, made by almost isolated $SnBr_3$ units characterized by very short Sn-Br distances.

Metal-halide perovskites containing the formamidinium (FA) A-site cation, in particular $FAPbBr_3$, have attracted significant interest both for the realization of perovskites solar cells and in the preparation of highly emitting nanocrystals.[1-10] The presence of the larger FA cation, with respect to methylammonium (MA), imparts the perovskite with several interesting properties: i) stabilization of the cubic perovskite phase at room temperature in the mixed MA/FA systems; ii) extension of the absorption edge towards the near-IR; iii) improvement of the thermal and humidity stability of PSCs and nanocrystals; and iv) enhancement of the carrier lifetime. [5-9, 11] Most of the FA-based perovskites reported in the literature are lead halides, while few information are available when exploring the substitution of Sn for Pb in such compounds. This is an argument of great actual interest because of the debated presence of environmental unfriendly Pb in perovskites; and because of the tuneable band-gap which can be achieved when alloying Pb and Sn in mixed ASn/PbX_3 perovskites.[12-15] Together with Sn/Pb perovskites, pure solar cells based on tin halides have been extensively fabricated and showed promising efficiencies, with the most performing devices obtained by using a mixed cation $FA_{0.75}MA_{0.25}SnI_3$ composition.[16] The stability of Sn(II) in a working device is a challenge, but it is believed that the current research activities will be able to quickly move towards a solution.[17]

Some of us have previously investigated the role of Sn doping on the $MAPbBr_3$ perovskite through the synthesis and characterization of the $MAPb_{1-x}Sn_xBr_3$ solid solution, showing a progressive reduction of the band-gap from 2.20 eV in $MAPbBr_3$ to about 1.33 eV in $MASnBr_3$.[18] This is the expected monotonic reduction of the band-gap upon increasing the Sn fraction predicted by modeling.[14] On the other hand, a more recent study on the $FA_{1-x}MA_xSnBr_3$ mixed system, revealed an unusual and unexpected trend in the evolution of the band-gap as a function of the organic cation.[19] In particular, it was observed that starting from $FASnBr_3$ the band-gap value progressively decreased from about 2.4 eV ($x = 0$) down to ~1.92 eV ($x = 0.82$), *i.e.* by about 0.5 eV, followed by an up-turn to about 2.0 eV for $MASnBr_3$, which

is, overall, a huge energy variation for a simple organic cation replacement. Indeed, such high variations are usually observed for B-cation or X-anion substitutions.[14, 18, 20] The results reported on the $FA_{1-x}MA_xSnBr_3$ solid solution seem to confirm the key role of structural distortions induced by A-site cations on the perovskite optical properties.[11]

Motivated by these results, indicating a possible new scenario in the electronic structure evolution of FA-based tin halides, by the great appeal of $FAPbBr_3$ for both photovoltaics and optoelectronic devices, and by the interest towards the replacement of Pb with Sn, we undertook a joint experimental and computational investigation of the $FAPb_{1-x}Sn_xBr_3$ system (*i.e.*, $0 \leq x \leq 1$). We have found a non monotonic band-gap evolution with the Sn content. The pure $FASnBr_3$ perovskite shows a higher band-gap than the corresponding $FAPbBr_3$ compound, with intermediate compositions showing a lower band-gap than $FAPbBr_3$. Surprisingly, the high band-gap of $FASnBr_3$ turns out to be the result of dynamical averaging of a quasi 0D structure, made by almost isolated $SnBr_3$ units characterized by very short Sn-Br distances, similar to the reported rhombohedral structure for $FAGeI_3$.[21] This is the result of the FA cation being too large to fit into the $SnBr_3$ cavity, and of the high-lying Sn *5s* orbitals strongly contributing to the top of the valence band in tin halide perovskites. Notably, this distortion is lifted in the $FAPbBr_3$ perovskite due to the lower energy of Pb *6s* orbitals, with $FASnBr_3$ probably representing the boundary compound of the 3D tin-halide perovskites domain.

The bulk $FAPb_{1-x}Sn_xBr_3$ samples were synthesized and characterized according to the methods reported in the Supporting Information. $FAPbBr_3$ crystallizes in a cubic space group at room temperature (*Pm*-3*m*) and undergoes two phase transitions (cubic to tetragonal between 275 and 250 K and tetragonal to orthorhombic between 150 and 125 K) by lowering the temperature.[22] $FASnBr_3$ also presents a cubic *Pm*-3*m* symmetry at room temperature, thus anticipating the possible existence of mixed Sn/Pb systems.[19]

The room temperature laboratory X-ray diffraction patterns of the samples of the $FAPb_{1-x}Sn_xBr_3$ system investigated in the present work are shown in Figure 1 where *x* values refer to the effective Sn/Pb composition determined by energy-dispersive X-ray spectroscopy (see the Experimental Section).

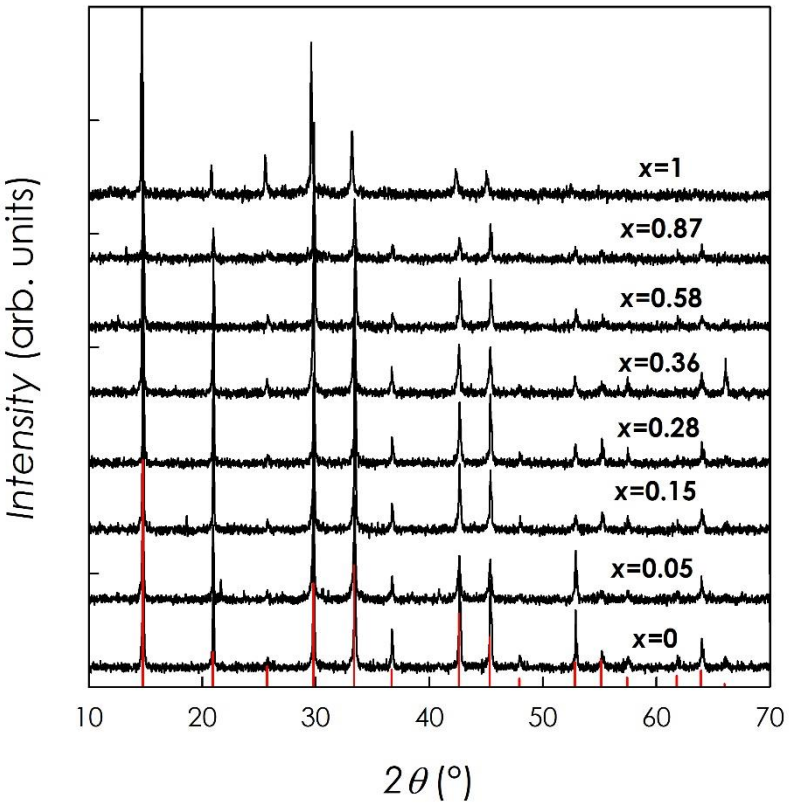

Figure 1. XRD patterns for the samples of the $FAPb_{1-x}Sn_xPbBr_3$ system. Patterns are vertically shifted to clarify viewing. Red vertical bars refer to the reflection positions for cubic structure (*Pm-3m*).

All the patterns reported in Figure 1 display the typical reflections of the cubic structure of metal-halide perovskites (*Pm*-3*m* – vertical red bars) and are free from detectable impurities. A slight peak broadening can be observed by increasing the Sn-content, as also found in previous Pb/Sn systems, but all the samples retain a high level of crystallinity.[18-19] By analogy with $FAGeI_3$ we cannot rule out a slight trigonal distortion,[21] which however cannot be

distinguished at the current level of XRD resolution. The cubic lattice parameter and cell volume determined from the refinement of the patterns are reported in Table 1.

Table 1. Lattice parameters (*a*, Å) and cell volumes (V, Å^3) for the investigated $FAPb_{1-x}Sn_xBr_3$ samples as a function of the Sn content (*x*).

x	*a*	*V*
0.00	5.9953(2)	215.50(1)
0.05	5.9946(2)	215.42(1)
0.15	5.9979(2)	215.78(1)
0.28	5.9976(2)	215.74(1)
0.36	5.9966(2)	215.64(1)
0.58	5.9970(2)	215.68(1)
0.87	6.0076(2)	216.82(1)
1.00	6.0344(2)	219.74(1)

The cell parameter and volume of the $FAPb_{1-x}Sn_xBr_3$ system remains substantially constant up to about *x*=0.58 where it starts increasing with a further relevant expansion for *x*=1, *i.e.* for the pure $FASnBr_3$ compound. This is an anomalous behavior with respect to other Pb/Sn mixed halide perovskites where a slight decrease of the cell volume by increasing the Sn-content has been reported,[18, 23] also according to the small ionic radius difference between Sn^{2+} and Pb^{2+} (0.97 and 1.03 Å, respectively).[24] Since the samples are single phase and the actual Sn/Pb content has been determined experimentally the results about the structural parameters

suggest that some level of distortion could be present also for an averagely cubic structure and that this distortion should manifest itself with a peculiar trend by increasing the Sn-content above x=0.50.

Related to the structural evolution, the $FAPb_{1-x}Sn_xBr_3$ system shows a correspondingly anomalous band-gap trend upon varying the Pb/Sn ratio. Figure 2a reports diffuse reflectance spectra and Figure 2b reports the extrapolated band-gap values as a function of the Sn-content. The band-gaps have been obtained from the extrapolation of the linear part of $[F(R)\ h\nu]^2$ where F(R) is the Kubelka-Munk function $F(R) = (1-R)^2/2R$.[25-26]

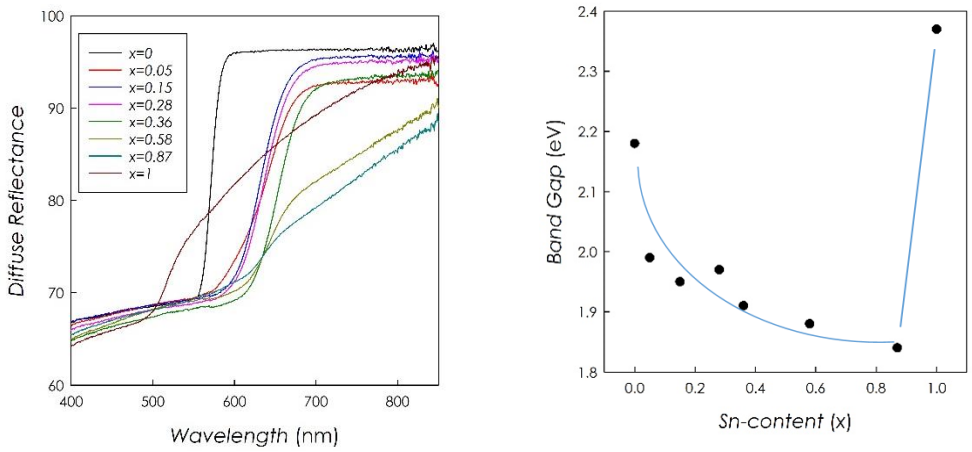

Figure 2. a) Diffuse reflectance spectra for the $FAPb_{1-x}Sn_xBr_3$ system. b) Band-gap trend as a function of Sn content (x).

From Figure 2a one observes a progressive shift of the fundamental absorption edge towards lower energies by replacing Sn on the Pb-site up to x=0.87, together with a reduction of the overall reflectance of the samples and a broadening of the absorption lineshape, which may be partially due to the increased and broadened absorption coefficient spectrum with increasing the Sn content.[14] An abrupt shift of the absorption edge towards higher energy is instead found for $FASnBr_3$. The band-gap value (Figure 2b) shows a progressive reduction by increasing x from about 2.18 eV ($FAPbBr_3$) to 1.84 eV (x=0.87), followed by a sudden upturn for $FASnBr_3$

(2.37 eV). Again, such behavior is anomalous and intriguing since in mixed Pb/Sn systems one would expect a monotonic band-gap variation with increasing the Sn content,[14] as experimentally found by Ogomi et al.[12] Hao et al.[13], however, observed an anomalous band-gap behavior by varying the Pb/Sn ratio in $MASn_{(1-x)}Pb_xI_3$ with intermediate compositions (x = 0.25 and 0.50) showing the lowest band-gap.

To gain insight into the reasons underlying the anomalous band-gap evolution with Pb/Sn alloying we have carried out hybrid DFT calculations including spin-orbit coupling (SOC). We relaxed both atomic positions and cell parameters by PBE,[27] followed by single point hybrid calculations including SOC using the modified version of the HSE06 functional[28] including 43% Hartree-Fock exchange proposed in Ref. [29]. This approach is found to correctly reproduce the results of GW calculations for both Pb and Sn compounds.[30]

We start our analysis by looking at results obtained for cubic 2x2x2 supercell. Atomic positions are allowed to relax keeping the experimental cell parameter fixed. No significant differences in electronic structure parameters are noted when relaxing the cell parameters, see Supporting Information (Table S1), thus we refer to experimental cell parameters for simplicity. For the mixed $FAPb_{0.50}Sn_{0.50}Br_3$ compound we explored several possible arrangements of the four Sn and Pb ions, see Supporting Information Figure S1 and Table S2, here we just refer to the most stable structure. A summary of the calculated structural and electronic features of the investigated species is reported in Table 2.

Table 2. Comparison between calculated and experimental band-gap (E_g, eV) for the cubic phase of $FAPb_{1-x}Sn_xBr_3$ perovskites as a function of the Sn/Pb ratio.

	E_g (eV)	
	Theor.	Exp.
$FAPbBr_3$	2.12	2.18

$FAPb_{0.50}Sn_{0.50}Br_3$	1.94	1.88 (x= 0.58)
$FASnBr_3$	2.49	2.37

As one may notice, the calculated band-gaps are in excellent agreement with experimental values. In line with experiments, we predict a decrease of the band-gap when moving to x = 0.5, to then increase again for the pure $FASnBr_3$ perovskite. The calculated band-gap trend can be explained by looking at the Density of States (DOS) reported in Figure 3. Introduction of Sn in $FAPb_{0.50}Sn_{0.50}Br_3$ stabilizes the conduction band minimum (CBM), with mixed Pb *6p* / Sn *5p* character, while the valence band maximum (VBM) remains essentially unaltered. Upon further increasing the Sn content the CBM is totally constituted by Sn *5p* orbitals and shifts at higher energy. Concomitantly, the VBM shifts at higher energy, as a result of the mixing between Sn *5s* and Br *4p* states, but the VBM shift is smaller than the CBM shift so, overall, the band-gap increases. This is at variance with the $MAPb_{1-x)}Sn_xI_3$ perovskites, where the VBM upshift was significantly larger than the CBM upshift leading to a significant band-gap reduction in $MASnI_3$ compared to $MAPbI_3$. [30]

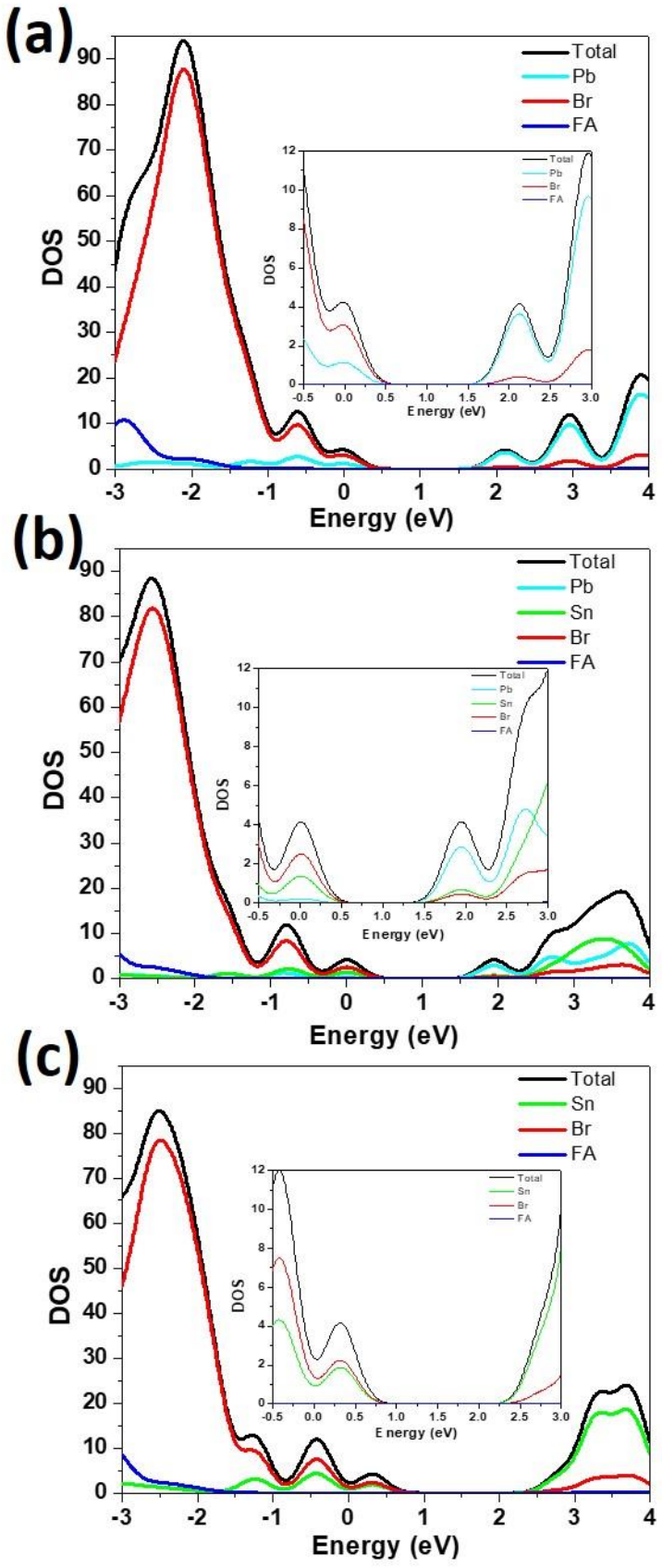
(a)
Total
Pb
Br
FA
DOS
Energy (eV)
(b)
Total
Pb
Sn
Br
FA
DOS
Energy (eV)
(c)
Total
Sn
Br
FA
DOS
Energy (eV)

Figure 3. Density of states (DOS) of cubic (a) $FAPbBr_3$, (b) $FAPb_{0.50}Sn_{0.50}Br_3$ (d) and (c) $FASnBr_3$ as calculated by HSE06-SOC. Valence band maxima has been set to zero in (a) and (b) and (c) have been aligned to the lowest carbon DOS peak.

To further investigate the origin of the band-gap evolution we inspected the optimized structures in Figure 4. $FASnBr_3$ was found to exhibit a strong long-short alternation of Sn-Br distances (2.76 vs. 3.30 Å), which gradually equalize when moving to $FAPb_{0.50}Sn_{0.50}Br_3$ (2.98 and 3.04 Å) and $FAPbBr_3$ (3.02 and 3.03 Å). While long-short alternation of apical metal halide distances is typical of tetragonal Sn- and Pb-halide perovskites,[14, 30] the calculated difference found in $FASnBr_3$ (~0.5 Å) is outstanding. Notably, such structural distortion is not related to a specific crystallographic direction but it is symmetrically distributed along the three crystal axes, see Figure 4 and Table 3, at variance with the long-short bond alternation along the [001] direction found in tetragonal metal-halide perovskites.[30] The structural distortion, leading to a polar structure similar to that reported for $FAGeI_3$,[21] actually drives the system towards a quasi-0D perovskite phase, since $SnBr_3$ units with short Sn-Br distances are separated by longer Sn-Br or Pb-Br distances from other units, see Figure 4b and 4c.

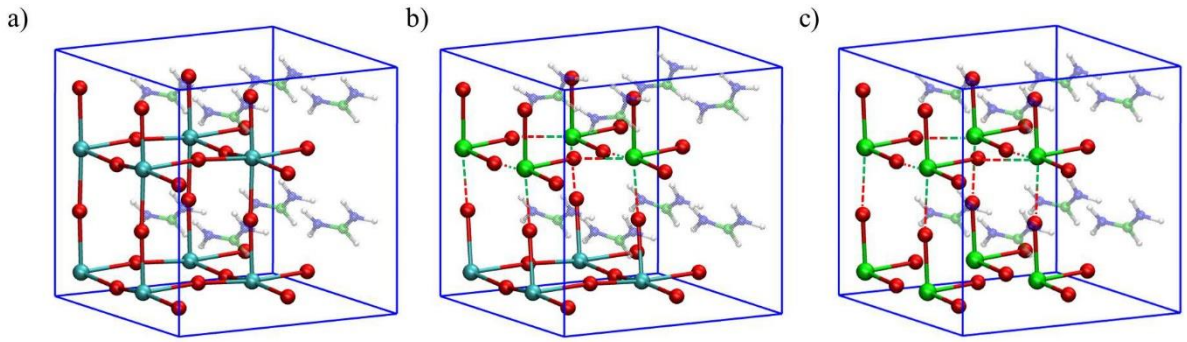

Figure 4. Optimized structures of cubic (a) $FAPbBr_3$, (b) $FAPb_{0.50}Sn_{0.50}Br_3$ (d) and (c) $FASnBr_3$. The dashed lines indicate long Sn-Br distances. Pb=light blue; I=red, Sn=green. FA molecules are shaded in the background for clarity.

To understand the reason underlying the large metal-halide bond alternation of $FASnBr_3$ we simulated a series of cubic perovskites, varying A (FA, MA, Cs), M (Ge, Sn, Pb) and X (Br, I), see Table 3. Notably a clear trend emerges, with the A-site cation modulating the distortion in $ASnBr_3$ perovskites; larger cations give larger distortions, with $CsSnBr_3$ being almost perfectly symmetric. The structural distortion has important consequences for the $ASnBr_3$ perovskites band-gap, which decreases from ~2.4 to ~1.7 eV across the FA $\rightarrow$ MA $\rightarrow$ Cs series. The observed structural asymmetry is partly lifted in $ASnI_3$ perovskites, with the largest deviation of the series (3.07 and 3.21 Å) being again observed for the $FASnI_3$ perovskite. The structural asymmetry is further reduced in $APbX_3$ perovskites, with a consequent band-gap leveling, see Table 3. Notably, in $AGeI_3$ perovskites the structural distortion was present even for $CsGeI_3$, characterized by short-long distances of 2.75-3.26 Å, and it further increased moving to larger cations, up to 2.73-3.58 Å in $FAGeI_3$.[21] Taken altogether this data seem to suggest a typical tolerance factor argument,[31-33] with the smaller tin bromide (and germanium iodide) perovskites being more sensitive to the size of the A-cations than lead halide and tin iodide compounds.

Table 3. Calculated short-long metal-halide bond lengths (Å) and experimental band-gaps (E_g, eV) for a series of cubic perovskites varying A, M and X. Cell parameters (see Supporting Information) and band-gaps are taken from the corresponding references. Calculated data are compared to experimental data for $AGeI_3$ perovskites.[21]

A	M	X	[100]	[010]	[001]	Avg.	E_g
FA	Sn	Br	2.81, 3.24	2.76, 3.30	2.80, 3.24	2.79, 3.26	2.37
MA	Sn	Br	2.81, 3.09	2.83, 3.08	2.83, 3.08	2.82, 3.08	2.00[a]
Cs	Sn	Br	2.88, 2.92	2.87, 2.93	2.87, 2.93	2.87, 2.93	1.75[b]
FA	Sn	I	3.09, 3.18	3.02, 3.28	3.09, 3.18	3.07, 3.21	1.41[c]
MA	Sn	I	3.03, 3.20	3.02, 3.23	3.02, 3.23	3.02, 3.22	1.20[c]
Cs	Sn	I	3.07, 3.13	3.06, 3.14	3.06, 3.14	3.06, 3.14	1.27[d]
FA	Pb	Br	3.00, 3.00	3.02, 3.03	2.98, 3.02	3.00, 3.02	2.18
MA	Pb	Br	2.94, 2.99	2.93, 3.02	2.92, 3.02	2.93, 3.01	2.20[e]
FA	Pb	I	3.19, 3.21	3.16, 3.22	3.20, 3.24	3.18, 3.22	1.48[c]
MA	Pb	I	3.16, 3.18	3.10, 3.25	3.10, 3.25	3.12, 3.23	1.52[c]
FA	Ge	I	-	-	-	2.75, 3.26	2.2[f]
MA	Ge	I	-	-	-	2.77, 3.45	1.9[f]
Cs	Ge	I	-	-	-	2.73, 3.58	1.6[f]

[a] Ref. [19]; [b] Ref. [34]; [c] Ref. [35]; [d] Ref. [23]; [e] Ref. [18]; [f] Ref. [21]

The observed structural distortion is apparently not consistent with the reported cubic phase of the investigated perovskites. Notice, however, that dynamical average may lead to an overall cubic structure, similar to the dynamically averaged cubic structure of $MAPbI_3$,[36] where the nominally cubic structure is actually the average of two distorted tetragonal structures. To check this point we have carried out *ab initio* molecular dynamics simulations on a 3x3x3 cubic $FASnBr_3$ supercell by means of the Car-Parrinello method,[37-38] setting the temperature at 350 K. We looked at the structural evolution of a set of Sn-Br distances spanning the [100], [010] and [001] directions against their global average during the dynamics. We report in Figure 5 the results for the [001] direction, similar data for the [100] and [010] directions can be found in Supporting Information, Figure S2.

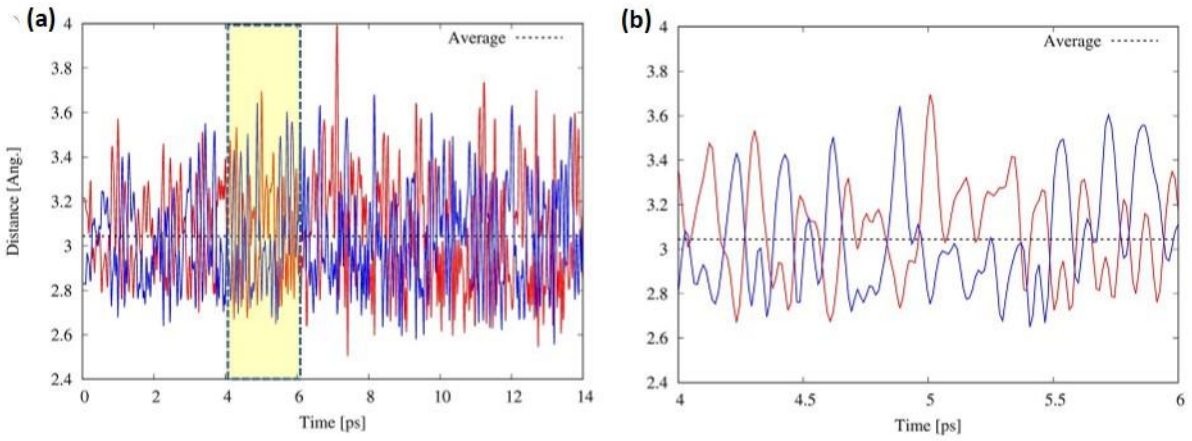

Figure 5. Time evolution of Sn-Br bond distances for a selected Sn center along the [001] direction. The right panel shows a detail of the time from 4 to 6 ps highlighted by the yellow rectangle on the left panel.

As it can be noticed, the average of the Sn-Br distances during the dynamics (3.04 Å) matches the average of the long and short distances calculated by structural optimizations. Furthermore, and more importantly, Figure 5b clearly shows that long Sn-Br bonds become short and viceversa within a typical time of ~0.15 ps. Thus, the structure is indeed averagely cubic, though it is instantaneously distorted. This implies that on the long time scale of structural characterizations, *e.g.* XRD, the structure is overall cubic, while on the short time scale of electronic transitions, *i.e.* upon resonantly exciting the material during absorption measurements, the structure is distorted delivering an increased band-gap value. This is confirmed by investigating the band-gap variation against a collective distortion parameter, see Supporting Information, Figure S3, so that the average band-gap is actually larger than the band-gap of the average structure.[36] Similar analysis performed on $FAGeI_3$ revealed a more pronounced barrier across the double well profile (0.06 vs 0.01 eV), suggesting that this system might be trapped in the distorted well for sufficient time to be observed through structural determination, see Figure S4.

To the best of our knowledge, $FASnBr_3$ (and to some extent $MASnBr_3$) are the first examples of such 3D perovskites originated by dynamical averaging of quasi-0D perovskites. As such, $FASnBr_3$ likely represents the boundary compound in the compositional space of 3D perovskites

Conclusions

We experimentally and theoretically investigated the $FAPb_{1-x}Sn_xBr_3$ system (*i.e.*, $0 \leq x \leq 1$). We have found a non monotonic band-gap evolution while changing the Sn content. In particular, the $FASnBr_3$ material shows a higher band-gap than the corresponding $FAPbBr_3$ compound, with intermediate compositions showing a lower band-gap than $FAPbBr_3$. This is due to the FA cation being too large to fit into the $SnBr_3$ cavity and inducing a quasi 0D structure. We further demonstrated by means molecular dynamics simulation that the high band-gap of $FASnBr_3$ turns out to be the result of dynamical averaging of a quasi 0D structure, constituted by almost isolated $SnBr_3$ units characterized by a short Sn-Br distances, similar to the reported rhombohedral structure for $FAGeI_3$.[21] However, we found that the kinetics barrier for the short/long M-X distance inversion is higher in $FAGeI_3$ with respect to $FASnBr_3$ suggesting that $FAGeI_3$ might be trapped in the distorted well for sufficient time to be observed through structural determination. In conclusion, $FASnBr_3$ is the first example of such 3D perovskite originated by dynamical averaging of quasi-0D material representing the boundary compound in the compositional space of 3D perovskites.

Supporting Information

Supporting Information Available: Experimental and Computational details.

.

Acknowledgement

The authors gratefully acknowledge the project PERSEO-"PERrovskite-based Solar cells: towards high Efficiency and lOng-term stability" (Bando PRIN 2015-Italian Ministry of University and Scientific Research (MIUR) Decreto Direttoriale 4 novembre 2015 n. 2488, project number 20155LECAJ) for funding.

References:

(1) Jeon, N. J.; Noh, J. H.; Yang, W. S.; Kim, Y. C.; Ryu, S.; Seo, J.; Seok, S. I. Compositional engineering of perovskite materials for high-performance solar cells. *Nature* **2015**, *517*, 476-480.
(2) Pellet, N.; Gao, P.; Gregori, G.; Yang, T.-Y.; Nazeeruddin, M. K.; Maier, J.; Grätzel, M. Mixed-Organic-Cation Perovskite Photovoltaics for Enhanced Solar-Light Harvesting. *Angew. Chem. Int. Ed.* **2014**, *53*, 3151-3157.
(3) Jesper Jacobsson, T.; Correa-Baena, J.-P.; Pazoki, M.; Saliba, M.; Schenk, K.; Gratzel, M.; Hagfeldt, A. Exploration of the compositional space for mixed lead halogen perovskites for high efficiency solar cells. *Energy Environ. Sci.* **2016**, *9*, 1706-1724.
(4) Yang, W. S.; Noh, J. H.; Jeon, N. J.; Kim, Y. C.; Ryu, S.; Seo, J.; Seok, S. I. High-performance photovoltaic perovskite layers fabricated through intramolecular exchange. *Science* **2015**, *348*, 1234-1237.
(5) Arora, N.; Dar, M. I.; Abdi-Jalebi, M.; Giordano, F.; Pellet, N.; Jacopin, G.; Friend, R. H.; Zakeeruddin, S. M.; Grätzel, M. Intrinsic and Extrinsic Stability of Formamidinium Lead Bromide Perovskite Solar Cells Yielding High Photovoltage. *Nano Lett.* **2016**, *16*, 7155-7162.
(6) Cho, K. T.; Paek, S.; Grancini, G.; Roldan-Carmona, C.; Gao, P.; Lee, Y.; Nazeeruddin, M. K. Highly efficient perovskite solar cells with a compositionally engineered perovskite/hole transporting material interface. *Energy Environ. Sci.* **2017**, *10*, 621-627.
(7) Pisanu, A.; Ferrara, C.; Quadrelli, P.; Guizzetti, G.; Patrini, M.; Milanese, C.; Tealdi, C.; Malavasi, L. The FA1–xMAxPbI3 System: Correlations among Stoichiometry Control, Crystal Structure, Optical Properties, and Phase Stability. *J. Phys. Chem. C* **2017**, *121*, 8746-8751.
(8) Zhumekenov, A. A.; Saidaminov, M. I.; Haque, M. A.; Alarousu, E.; Sarmah, S. P.; Murali, B.; Dursun, I.; Miao, X.-H.; Abdelhady, A. L.; Wu, T., et al. Formamidinium Lead Halide Perovskite Crystals with Unprecedented Long Carrier Dynamics and Diffusion Length. *ACS Energy Lett.* **2016**, *1*, 32-37.
(9) Minh, D. N.; Kim, J.; Hyon, J.; Sim, J. H.; Sowlih, H. H.; Seo, C.; Nam, J.; Eom, S.; Suk, S.; Lee, S., et al. Room-Temperature Synthesis of Widely Tunable Formamidinium Lead Halide Perovskite Nanocrystals. *Chem. Mater.* **2017**, *29*, 5713-5719.

(10) Protesescu, L.; Yakunin, S.; Bodnarchuk, M. I.; Bertolotti, F.; Masciocchi, N.; Guagliardi, A.; Kovalenko, M. V. Monodisperse Formamidinium Lead Bromide Nanocrystals with Bright and Stable Green Photoluminescence. *J. Am. Chem. Soc.* **2016**, *138*, 14202-14205.
(11) Amat, A.; Mosconi, E.; Ronca, E.; Quarti, C.; Umari, P.; Nazeeruddin, M. K.; Grätzel, M.; De Angelis, F. Cation-Induced Band-Gap Tuning in Organohalide Perovskites: Interplay of Spin–Orbit Coupling and Octahedra Tilting. *Nano Lett.* **2014**, *14*, 3608-3616.
(12) Ogomi, Y.; Morita, A.; Tsukamoto, S.; Saitho, T.; Fujikawa, N.; Shen, Q.; Toyoda, T.; Yoshino, K.; Pandey, S. S.; Ma, T., et al. CH3NH3SnxPb(1–x)I3 Perovskite Solar Cells Covering up to 1060 nm. *J. Phys. Chem. Lett.* **2014**, *5*, 1004-1011.
(13) Hao, F.; Stoumpos, C. C.; Chang, R. P. H.; Kanatzidis, M. G. Anomalous Band Gap Behavior in Mixed Sn and Pb Perovskites Enables Broadening of Absorption Spectrum in Solar Cells. *J. Am. Chem. Soc.* **2014**, *136*, 8094-8099.
(14) Mosconi, E.; Umari, P.; De Angelis, F. Electronic and optical properties of mixed Sn-Pb organohalide perovskites: a first principles investigation. *J. Mater. Chem. A* **2015**, *3*, 9208-9215.
(15) Eperon, G. E.; Leijtens, T.; Bush, K. A.; Prasanna, R.; Green, T.; Wang, J. T.-W.; McMeekin, D. P.; Volonakis, G.; Milot, R. L.; May, R., et al. Perovskite-perovskite tandem photovoltaics with optimized band gaps. *Science* **2016**, *354*, 861-865.
(16) Zhao, Z.; Gu, F.; Li, Y.; Sun, W.; Ye, S.; Rao, H.; Liu, Z.; Bian, Z.; Huang, C. Mixed‐Organic‐Cation Tin Iodide for Lead‐Free Perovskite Solar Cells with an Efficiency of 8.12%. *Adv. Sci.* **2017**, *4*, 1700204.
(17) Abate, A. Perovskite Solar Cells Go Lead Free. *Joule 1*, 887.
(18) Mancini, A.; Quadrelli, P.; Milanese, C.; Patrini, M.; Guizzetti, G.; Malavasi, L. CH3NH3SnxPb1–xBr3 Hybrid Perovskite Solid Solution: Synthesis, Structure, and Optical Properties. *Inorg. Chem.* **2015**, *54*, 8893-8895.
(19) Ferrara, C.; Patrini, M.; Pisanu, A.; Quadrelli, P.; Milanese, C.; Tealdi, C.; Malavasi, L. Wide band-gap tuning in Sn-based hybrid perovskites through cation replacement: the FA1-xMAxSnBr3 mixed system. *J. Mater. Chem. A* **2017**, *5*, 9391-9395.
(20) Borriello, I.; Cantele, G.; Ninno, D. Ab initio investigation of hybrid organic-inorganic perovskites based on tin halides. *Phys. Rev. B* **2008**, *77*, 235214.
(21) Stoumpos, C. C.; Frazer, L.; Clark, D. J.; Kim, Y. S.; Rhim, S. H.; Freeman, A. J.; Ketterson, J. B.; Jang, J. I.; Kanatzidis, M. G. Hybrid Germanium Iodide Perovskite Semiconductors: Active Lone Pairs, Structural Distortions, Direct and Indirect Energy Gaps, and Strong Nonlinear Optical Properties. *J. Am. Chem. Soc.* **2015**, *137*, 6804-6819.
(22) Schueller, E. C.; Laurita, G.; Fabini, D. H.; Stoumpos, C. C.; Kanatzidis, M. G.; Seshadri, R. Crystal Structure Evolution and Notable Thermal Expansion in Hybrid Perovskites Formamidinium Tin Iodide and Formamidinium Lead Bromide. *Inorg. Chem.* **2018**, *57*, 695-701.
(23) Sabba, D.; Mulmudi, H. K.; Prabhakar, R. R.; Krishnamoorthy, T.; Baikie, T.; Boix, P. P.; Mhaisalkar, S.; Mathews, N. Impact of Anionic Br– Substitution on Open Circuit Voltage in Lead Free Perovskite (CsSnI3-xBrx) Solar Cells. *J. Phys. Chem. C* **2015**, *119*, 1763-1767.
(24) Becker, M.; Kluner, T.; Wark, M. Formation of hybrid ABX3 perovskite compounds for solar cell application: first-principles calculations of effective ionic radii and determination of tolerance factors. *Dalton Trans.* **2017**, *46*, 3500-3509.
(25) Kubelka, P.; Munk, F. Ein Beitrag zur Optik der Farbanstriche. *Zeit. Fur Tekn. Physik* **1931**, *12*, 593-601.
(26) Kim, H.-S.; Lee, C.-R.; Im, J.-H.; Lee, K.-B.; Moehl, T.; Marchioro, A.; Moon, S.-J.; Humphry-Baker, R.; Yum, J.-H.; Moser, J. E., et al. Lead Iodide Perovskite Sensitized All-Solid-State Submicron Thin Film Mesoscopic Solar Cell with Efficiency Exceeding 9%. *Sci. Rep.* **2012**, *2*, 591.

(27) Perdew, J. P.; Burke, K.; Ernzerhof, M. Generalized Gradient Approximation Made Simple. *Phys. Rev. Lett.* **1996**, *77*, 3865-3868.
(28) Heyd, J.; Scuseria, G. E.; Ernzerhof, M. Hybrid functionals based on a screened Coulomb potential. *J. Chem. Phys.* **2003**, *118*, 8207-8215.
(29) Du, M.-H. Density Functional Calculations of Native Defects in CH3NH3PbI3: Effects of Spin–Orbit Coupling and Self-Interaction Error. *J. Phys. Chem. Lett.* **2015**, *6*, 1461-1466.
(30) Umari, P.; Mosconi, E.; De Angelis, F. Relativistic GW calculations on $CH_3NH_3PbI_3$ and $CH_3NH_3SnI_3$ Perovskites for Solar Cell Applications. *Sci. Rep.* **2014**, *4*, 4467.
(31) Kieslich, G.; Sun, S.; Cheetham, A. K. Solid-state principles applied to organic-inorganic perovskites: new tricks for an old dog. *Chem. Sci.* **2014**, *5*, 4712-4715.
(32) Travis, W.; Glover, E. N. K.; Bronstein, H.; Scanlon, D. O.; Palgrave, R. G. On the application of the tolerance factor to inorganic and hybrid halide perovskites: a revised system. *Chem. Sci.* **2016**, *7*, 4548-4556.
(33) Gholipour, S.; Ali, A. M.; Correa-Baena, J.-P.; Turren-Cruz, S.-H.; Tajabadi, F.; Tress, W.; Taghavinia, N.; Grätzel, M.; Abate, A.; De Angelis, F., et al. Globularity-Selected Large Molecules for a New Generation of Multication Perovskites. *Adv. Mater.* **2017**, *29*, 1702005.
(34) Gupta, S.; Bendikov, T.; Hodes, G.; Cahen, D. CsSnBr3, A Lead-Free Halide Perovskite for Long-Term Solar Cell Application: Insights on SnF2 Addition. *ACS Energy Lett.* **2016**, *1*, 1028-1033.
(35) Stoumpos, C. C.; Malliakas, C. D.; Kanatzidis, M. G. Semiconducting Tin and Lead Iodide Perovskites with Organic Cations: Phase Transitions, High Mobilities, and Near-Infrared Photoluminescent Properties. *Inorg. Chem.* **2013**, *52*, 9019-9038.
(36) Quarti, C.; Mosconi, E.; Ball, J. M.; D'Innocenzo, V.; Tao, C.; Pathak, S.; Snaith, H. J.; Petrozza, A.; De Angelis, F. Structural and optical properties of methylammonium lead iodide across the tetragonal to cubic phase transition: implications for perovskite solar cells. *Energy Environ. Sci.* **2016**, *9*, 155-163.
(37) Car, R.; Parrinello, M. Unified Approach for Molecular Dynamics and Density-Functional Theory. *Phys. Rev. Lett.* **1985**, *55*, 2471-2474

(38) Giannozzi, P.; Angelis, F. D.; Car, R. First-principle molecular dynamics with ultrasoft pseudopotentials: Parallel implementation and application to extended bioinorganic systems. *J. Chem. Phys.* **2004**, *120*, 5903-5915.